J Solid State Electrochem (2006) 10: 96–103
DOI 10.1007/s10008-005-0667-5

ORIGINAL PAPER

J. R. Frade · V. V. Kharton
A. A. Yaremchenko · E. V. Tsipis

Applicability of emf measurements under external load resistance conditions for ion transport number determination

Received: 18 January 2005 / Revised: 19 February 2005 / Accepted: 8 March 2005 / Published online: 12 May 2005

Abstract In order to evaluate the applicability of concentration cells for the ion transference number measurements with external load, the cell response was simulated with variable transport properties of the cell material, external load resistance, geometrical factors such as ion-conducting membrane thickness, and electrode kinetics. This technique is expected to be pertinent when $\eta F/RT < 0.2$, except possibly for conditions when the electrode kinetics is dependent on a relatively small limiting current density. In each particular case, the method validity can be verified by testing if the overpotential sum grows faster than current on decreasing the external load resistance. A pyrochlore-type material $Gd_{1.9}Ca_{0.1}Ti_2O_{7-\delta}$ with dominant oxygen ionic conductivity is used as a study case to demonstrate the criteria proposed to assess the applicability of emf measurements under short-circuit conditions.

Keywords Transference number · Emf measurements · Mixed conductor · External load · Exchange current density

Introduction

Minor electronic conductivity affects the applicability of ionic conductors as solid electrolytes for fuel cells, potentiometric oxygen sensors, electrolysers or oxygen pumps and other electrochemical applications. Though major electronic contributions are often evaluated from the dependence of total conductivity on the partial pressure of oxygen, other methods are needed to determine minor contributions, such as the measurements of oxygen permeability, emf of concentration cells, Faradaic efficiency, isotopic exchange, or conductivity relaxation [1–12]. However, most of such techniques may still be affected by significant errors, and some authors [1, 2, 10, 11] thus proposed modified methods which take into account overpotential contributions. These methods are based on a modification of the equivalent circuit proposed by Patterson [13], with inclusion of the overpotential term η and with an external load resistance R_{ext} (Fig. 1). On assuming a nearly linear dependence of overpotential on ionic current (I), one can also express the effects of electrode overpotentials in terms of a polarisation resistance (R_η):

$$R_\eta = \frac{d\eta}{dI} \tag{1}$$

The equivalent circuit then yields:

$$\frac{E_o}{E} - 1 = [t_I^{-1} + (\sigma/L) \times AR_\eta][t_e + L/(A\sigma R_{ext})] = b + \frac{a \times L}{(A\sigma R_{ext})}, \tag{2}$$

where L is the cell thickness, A is the electrode area, $\sigma = \sigma_I + \sigma_e$ is the total conductivity equal to the sum of ionic (σ_I) and electronic (σ_e) contributions, $t_e = \sigma_e/\sigma$ is the electronic transport number, $t_I = (1\text{-}t_e)$ is the ion transport number, E is the measured emf, a and b are constants. In this equation, E_o is the Nernst potential generated by a chemical potential gradient in the cell. For an oxygen ion-conducting membrane placed under an oxygen chemical potential gradient:

$$E_o = \frac{RT}{4F} \times \ln\frac{pO_{2,ref}}{pO_2}, \tag{3}$$

where R is the ideal gas constant, T is absolute temperature, F is the Faraday constant, pO_2 and $pO_{2,ref}$ are the oxygen partial pressures at the cell electrodes. Equation 2 thus predicts a linear dependence

J. R. Frade (✉) · V. V. Kharton
A. A. Yaremchenko · E. V. Tsipis
Department of Ceramics and Glass Engineering,
CICECO, University of Aveiro,
3810-193 Aveiro, Portugal
E-mail: jfrade@cv.ua.pt
Tel.: +351-234-370254
Fax: +351-234-425300

(E_o/E)-1 = $b + aL/(A\sigma \quad R_{ext})$; the electronic transport number can be obtained on combining the values of the matching parameters, a and b, with the total conductivity of cell material, which can be determined, for example, by impedance spectroscopy. This technique was proposed by Gorelov [1] and later successfully used for the study of numerous mixed-conducting materials (e.g. [10, 12]).

The applicability of Eq. 2 may fail for highly polarisable electrodes, or when η vs. I deviates from the assumed linear relation. In this case, the polarisation resistance is not necessarily constant ($R_\eta \neq \eta/I$), and the cell response should be re-written as:

$$\frac{E_o}{E} - 1 = [t_I^{-1} + (\sigma/L)(\eta/i)][t_e + L/(A\sigma R_{ext})], \tag{4}$$

where $i = I/A$ is the current density. One thus expects arguments against the applicability of this method based on emf measurements under external load conditions [14]. The main objective of the present work was to re-examine conditions when the assumptions of linear behaviour are nearly true, and to obtain criteria to validate applicability of this method.

Formulation of the problem

One may simulate the dependence of overpotential versus current density for typical electrode kinetics to evaluate its effects on the emf reading and to identify conditions when Eq. 2 fails. From the equivalent circuit shown in Fig. 1 one obtains:

$$E = E_o - \frac{iL}{\sigma_I} - \eta. \tag{5}$$

On computing values of η and E, for given values of exchange current density, one can assess the applicability of Gorelov's method. The dependence of overpotential contributions on current density can be described by suitable kinetic relations such as the Buttler–Volmer equation, which describes charge transfer control. In this case, the current density versus overpotential relations for oxygen reduction and oxygen evolution are:

$$|i| = i_{oc}\exp[\alpha_c|\eta_c|n_cF/RT] - i_{oa}\exp[-(1-\alpha_c)|\eta_c|n_cF/RT] \tag{6}$$

and

$$i = i_{oa}\exp[(1-\alpha_a)\eta_a n_a F/RT] - i_{oc}\exp[-\alpha_a\eta_a n_a F/RT], \tag{7}$$

where the subscripts "c" and "a" correspond to cathode and anode processes, respectively, i_{oc} and i_{oa} are the exchange current density values for oxygen reduction at the feed side and oxygen evolution at the permeate side, α_c and α_a are the exchange coefficients, n_c and n_a represent the number of electrons participating in the electrode reactions.

The effect of current limitations is also widely known (e.g. [15, 16]), although the actual mechanisms for oxygen reduction are somewhat unclear, thus leading to differences in the models proposed by different authors. For control by diffusion of adsorbed oxygen atoms, Kenjo et al. [16] proposed:

$$|i| = i_o\{(1-|i/i_{Lc}|)^{1/2}\exp[2\alpha_c|\eta_c|F/RT] - \exp[-2(1-\alpha_c)|\eta_c|F/RT]\}, \tag{8}$$

where i_L is the limiting current density. Wang and Nowick [15] suggested another solution on assuming control by dissociative adsorption $O_2 + 2V_{ad} \rightarrow 2O_{ad}$:

$$|i| = i_o\{(1-|i/i_{Lc}|)\exp[\alpha_c|\eta_c|n_cF/RT] - \exp[-(1-\alpha_c)|\eta_c|n_cF/RT]\}. \tag{9}$$

A similar relation may be assumed to include current limitations in the permeate side, i.e. for the reaction of oxygen evolution. For the case of diffusion limitations, one thus assumes:

$$i = i_o\{(1-i/i_{La})^{1/2}\exp[(1-\alpha_a)\eta_a n_a F/RT] - \exp[-\alpha_a\eta_a n_a F/RT]\}. \tag{10}$$

In fact, one may anticipate strict limitations in electrode kinetics for cases when the atmosphere is very diluted, i.e., with low oxygen contents, as revealed by the failure of potentiometric oxygen sensors under such conditions [17]. This might be ascribed to a combination of decrease in exchange current density [15] and probably an even more drastic decrease in limiting current density with reducing oxygen partial pressure [17, 18]. Exchange current density results for ceria-based materials suggest a power law dependence,

$$i_o \propto (pO_2)^{1/4}, \tag{11}$$

at least for temperatures above 600 °C [19]. Cathodic overpotential corresponds to a drop in oxygen partial pressure on the feed side $\eta_c = (RT/F)\ln\ (pO_2/pO_{2,feed})^{1/4}$, (with $\eta_c < 0$) and thus

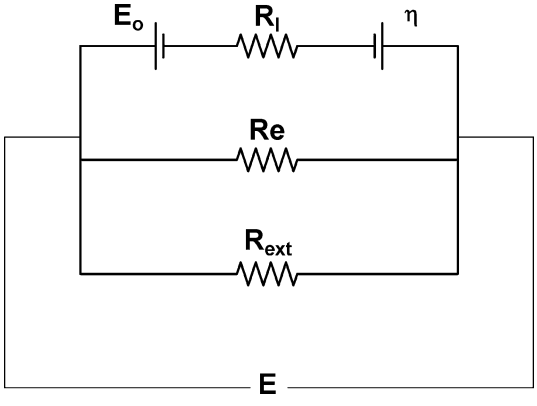

Fig. 1 Representation of the equivalent circuit. R_i and R_e are the partial ionic and electronic resistances

$$i_o = (i_{o,ref}) \times \exp[\eta_c F/RT], \quad (12)$$

where $i_{o,feed}$ is the exchange current density at feed side conditions $pO_{2,feed}$.

Very low values of pO_2 also imply limitations of mass transport in the gas phase, with oxygen flux $jO_2 = [D/(RT)](pO_2/\delta)$ and a limiting current density $i_L = 4FjO_2$. The latter quantity can be estimated considering typical values of the diffusion coefficient in the gas phase (D, about $\sim 10^{-4}$ m^2/s), a boundary layer thickness (δ, probably close to 10^{-3} m), and an oxygen partial pressure given by $pO_2 = (pO_{2,ref}) \times \exp[-4F(E_o - |\eta_c| - \eta_a)/RT)]$. At $T = 1{,}023$ K and $pO_{2,ref} = 21$ kPa, one expects i_L values in the order of 10^3, 11, 0.12, and 1.2×10^{-3} A/m^2 for $(E_o - |\eta_c| - \eta_a) = 0.1$, 0.2, 0.3 and 0.4 V, respectively. These limitations are probably critical at least for values of Nernst potential higher than about 0.2 V.

Equations 8 and 10 were used to obtain numerical solutions of η_a, and $|\eta_c|$, for given values of current density, with characteristic values of α_a, η_a, i_{La}, α_c, η_c and i_{Lc}. The values of i and $\eta = \eta_a + |\eta_c|$ were then calculated and used to obtain the corresponding emf values (E), and to evaluate the effects of transport properties of the cell material and external load resistance R_{ext}, Eq. 4.

Criteria to validate emf measurements

Linearity of $E_o/E-1$ versus $1/R_{ext}$ can be taken as a first criterion to confirm the applicability of emf measurements under short-circuit conditions. However, this can raise doubts due to scattering of experimental data, especially for cases when the ranges of $1/R_{ext}$ are relatively narrow. One should thus seek alternative criteria to assess the applicability of this method. For example, one may establish a criterion to verify the linearity of overpotential versus current. This approximation can be based on the expected linearisation of the exponential terms, i.e., $e^{\pm x} \approx 1 \pm x$, which is nearly true for sufficiently small values of x. Typically, one may use this condition for $x < 0.1$ with errors below approximately 5%, or $x < 0.2$ with errors up to 10%. On selecting a condition $x < 0.1$ and assuming that the electrode kinetics is controlled by charge transfer, Eqs. 6 and 7, one obtains $\alpha_a\ \eta_a\ n_a(F/RT) < 0.1$ and $\alpha_c|\eta_c|n_c(F/RT) < 0.1$, or $\eta_a\ n_a(F/RT) < 0.2$ and $|\eta_c|\ n_c(F/RT) < 0.2$ for typical values of charge transfer coefficients $\alpha_a \approx \alpha_c \approx 0.5$. Actually, it is usually difficult to test these criteria because the only information available in most cases is total overpotential sum η rather than the individual contributions η_a and $|\eta_c|$. One must thus rely on a single criterion based on the overall overpotential $\eta = \eta_a + |\eta c|$. Taking into account that typical values of n are often close to 2, the criterion is formulated as:

$$\frac{\eta F}{RT} < 0.2. \quad (13)$$

For example, one may express the overpotential as a function of emf readings, as given by the equivalent circuit of Fig. 1:

$$\eta = E_o - E[1 + (R_I/R_e) + (R_I/R_{ext})] = E_o - E[1 + (\sigma_e/\sigma_I) + (L/A)(\sigma_I R_{ext})^{-1}]. \quad (14)$$

In this case the criterion Eq. 13 becomes:

$$\{E_o - (E/t_I)[1 + 1/(\sigma R_{ext} A/L)]\}F/(RT) < 0.2. \quad (15)$$

The partial electronic resistance $R_e = L/A\sigma_e$, which can be extracted by matching of (E_o/E)-1 vs. $1/R_{ext}$ dependencies, may thus be combined with the experimental data of E vs. R_{ext}, to verify if the actual range of conditions fulfil the criterion of the nearly linear approximation (Eq. 15), thus validating the emf measurements under short-circuit conditions. One can easily recognize that this criterion is likely to be met for cells with nearly reversible electrodes, and re-write the applicability criterion in terms of exchange current density values for both electrodes. This can be obtained by inserting the linear approximation in Eqs. 6 and 7, resulting in:

$$\eta \approx i[(i_{oc}n_c)^{-1} + (i_{oa}n_a)^{-1}]RT/F \quad (16)$$

and

$$\eta F/RT \approx i[(i_{oa}n_a)^{-1} + (i_{oa}n_a)^{-1}] < 0.2. \quad (17)$$

The actual values of ionic leakage current depend on the ionic and electronic conductivities of the cell material and increase with decreasing external resistance. Hence, one should avoid excessively low values of external resistance to avoid undue increase in current density. A second advantage of using only large values of external resistance is to narrow the range of current values, and the corresponding changes in polarisation resistance, even for cases when the previous validity criterion (Eq. 13 or 15) might fail. For example, Eqs. 6 and 7 might still tend to Tafel-like approximations, $i \approx i_{oa}\exp[(1-\alpha_a)n_a\eta_a F/RT] \approx i_{oc}\exp(\alpha_c|\eta_c|n_c F/RT)$, for relatively large overpotential contributions, and one can use these Tafel dependences to obtain the dependence of polarisation resistance on current density:

$$R_\eta = d\eta/di = i^{-1}(RT/F)\{[(1-\alpha_a)n_a]^{-1} + (\alpha_c n_c)^{-1}\}. \quad (18)$$

This dependence is weak for conditions when the relative changes in current are small. Therefore, one may still assume a nearly constant polarisation resistance when the selected values of external resistance yield current densities in a relatively narrow range. However, the values of $1/R_{ext}$ must be sufficiently large to ensure good correlation for the plots of $E_o/E-1$ versus $1/R_{ext}$, providing meaningful fitting parameters and a correct determination of R_e.

The values of current $I = E(R_e^{-1} + R_{ext}^{-1})$ (see Fig. 1) can be evaluated after obtaining the value of R_e from the plot of $E_o/E-1$ versus $1/R_{ext}$. Alternatively, one can obtain the current density values on combining the conductivity, electronic transport number and external resistance:

$$i = (E/L)[\sigma t_e + L/(AR_{ext})] \quad (19)$$

The lowest current density value $i_{min} = E_{max}L/(\sigma\ t_e)$ is obtained for open-circuit conditions, and the maximum current is for the lowest emf reading. i.e.: $i_{max} = E_{min}[R_e^{-1} + (R_{ext,min})^{-1}]$. This yields a relative change

$$\Delta i/i_{min} = (E_{min}/E_{max})[1 + L/(\sigma t_e A R_{ext,min})] - 1. \quad (20)$$

Current limitations constitute additional reasons for concern about the applicability of emf measurements under short-circuit conditions. In this case, the overpotential rises sharply with relatively small increase in current values, invalidating the assumption of nearly constant polarisation resistance. One should thus examine the dependence of overpotential (Eq. 14) on current density (Eq. 19) to detect cases when a sharp increase in overpotential might indicate strict current limitations.

Simulations

A numerical method was used to calculate the values of η_a, and $|\eta_c|$, for a set of values of current density; the values of current and overpotential $\eta = \eta_a + |\eta_c|$ were then used to calculate the corresponding emf values, for given E_o, cell geometric parameters (thickness and area), transport properties of the cell material, and external resistance. Typical examples are shown in Figs. 2, 3, 4, 5.

The example shown in Fig. 2 was computed for the conditions given in Table 1. The open-circuit emf value computed for those conditions was $E/E_o = 0.902$, thus giving a very overestimated value of the electronic transport number $t_e^* = 1 - E/E_o = 0.098$. However, the dependence of $E_o/E-1$ vs $1/R_{ext}$ is nearly linear and the values of the slope/ intercept ratio give quite correct estimates of the electronic transport number, as illustrated in Fig. 2. This can be explained by taking into account that the values of $\eta F/RT$ remain lower than 0.2, thus validating the assumed nearly linear dependence of overpotential on current.

The open-circuit emf reading yields crude estimates of electronic transport number even for higher values of exchange current density (e.g. $1 - E/E_o = 0.044$ for the case when $t_e = 0.01$ and $i_{oc} = i_{oa} = 10^2$ A/m^2). Again, the corresponding results obtained from the slope/intercept ratio of $E_o/E-1$ vs $1/R_{ext}$ recover the correct values of electronic transport number in the whole range of t_e variations. Typical examples are shown in Fig. 3.

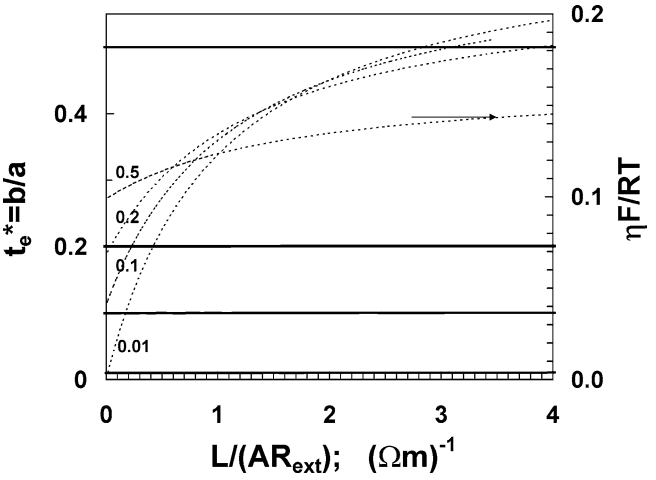

Fig. 3 Predictions of emf measurements under short-circuit conditions for different values of electronic transport number ($t_e = 0.01$, 0.1, 0.2 and 0.5). Other conditions are listed in Table 1

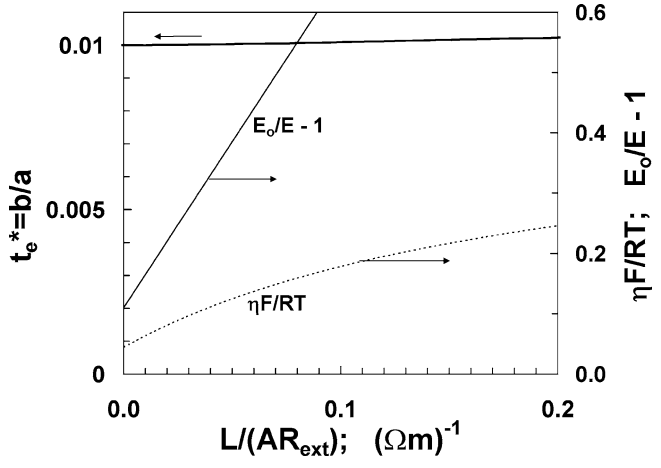

Fig. 2 Predictions of emf measurements under short-circuit conditions and for the conditions listed in Table 1

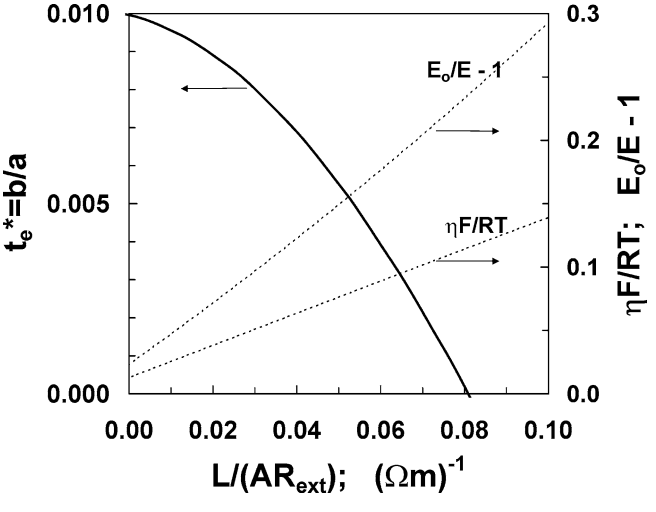

Fig. 4 Predictions for emf measurements under external load conditions with current density limitations $i_{La} = 10$ A/m^2, and other conditions listed in Table 1

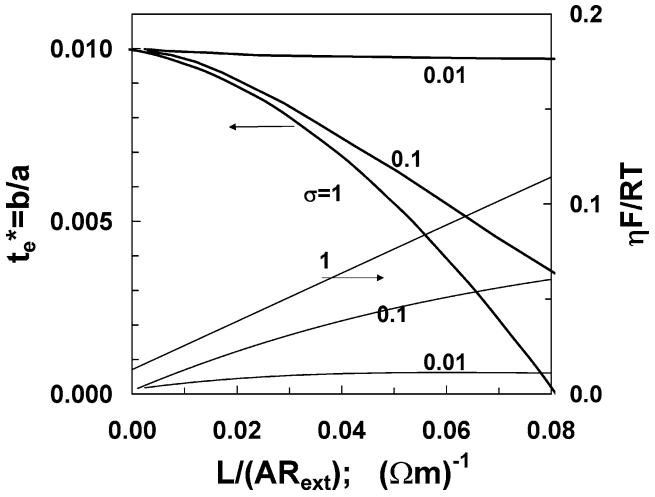

Fig. 5 Predictions for emf measurements under external load conditions with current density limitations $i_{La} = 10$ A/m^2, total conductivity of 0.01, 0.1, 1.0 (shown in the figure), and other conditions listed in Table 1

The effects of relatively strict current limitations are illustrated in Fig. 4. Though the values of dimensionless overpotential $\eta F/RT$ still remain lower than 0.2, the overpotential and the corresponding polarisation resistance values rise rapidly on approaching the limiting current density. The polarisation resistance is thus underestimated if assuming the linear approximation; this yields overestimated values of ionic transport number and underestimated t_e values. This may be shown by decreasing the external load resistance down to values lower than the overall resistance of the cell material when the internal leakage is determined mainly by the ionic conductivity. As shown in Fig. 4 low values of limiting current density and thus predominant current limitations tend to yield a curve of $E_o/E-1$ vs $1/R_{ext}$ which bends upwards, as opposed to the trend expected for a charge transfer mechanism.

When the emf results are affected by strict current limitations, one should also seek conditions when current limitations are less likely to occur. For example, decreasing temperatures may cause a greater decrease in ionic and electronic conductivities of the cell material than in the limiting current, especially when the latter is controlled by diffusion in a diluted gas phase. In this case, one increases the relative gap between the actual values of current and the limiting current. This type of effects has been illustrated by simulating the behaviour expected for different conductivities without changes in the limiting current (Fig. 5). The predictions show that such changes minimize the errors associated with relatively low current limits.

Figure 5 also shows that one should restrict the range of $L/(AR_{ext})$, which corresponds to establishing a lower limit for the values of external load resistance. A possible criterion to assess such a lower limit might be derived by imposing a typical condition of a narrow range of current density values, $\Delta i/i_{min} << 1$, to validate the applicability of the actual method, as discussed above. This should also correspond to a narrow range of values of E, and on combining with Eq. 20, we obtain a typical criterion for the lowest external load resistance:

$$R_{ext} >> L/(\sigma t_e A). \tag{21}$$

The load resistance must thus be sufficiently higher than the electronic resistance of the sample, as illustrated in Fig. 5. We therefore require estimates of the order of magnitude of the electronic resistance to select a suitable range of values of R_{ext}. Otherwise, we may assume a typical range of electronic transport number of the order of 0.01 for materials with predominantly ionic conductivity, thus obtaining a typical range suggested by the examples shown in Fig. 5, i.e.:

$$R_{ext} >> 100L/(\sigma A). \tag{22}$$

Table 1 Characteristic parameters used for simulations illustrated by Figs. 2, 3, 4, 5

Parameter	Fig. 2	Fig. 3	Fig. 4	Fig. 5
E_o (mV)	50	50	100	100
i_{oc} (A/m^2)	10	10^2	10^3	10^3
i_{oa} (A/m^2)	10	10^2	10^3	10^3
i_{Lc} (A/m^2)	∞	∞	∞	∞
i_{La} (A/m^2)	∞	∞	10	10
σ (S/m)	2	2	1	1, 0.1, 0.01
t_e	0.01	0.01–0.5	0.01	0.01

Other typical values were assumed for the remaining parameters, i.e.: $L = 2$ mm, $\alpha_c = \alpha_a = 0.5$, and $n_c = n_a = 2$

Study Case

The material selected to illustrate the applicability of emf measurements under external load conditions was pyrochlore-type $Gd_{1.9}Ca_{0.1}Ti_2O_{7-\delta}$. Its preparation, characterization of transport properties and assessment as a potential electrolyte for solid oxide fuel cells have been reported elsewhere [11]. The emf results are now re-examined to assess if they fulfil the applicability criteria proposed in the present work. In fact, the linearity of $E_o/E-1$ versus $1/R_{ext}$ is a first indication of the applicability of the method proposed to measure the transport numbers by emf measurements obtained under short-circuit conditions (Fig. 6). Transport numbers are shown in Fig. 7 (closed symbols) and differ clearly from the corresponding values obtained by open-circuit emf measurements (open symbols). These results correspond to average ionic transport number for values of oxygen partial pressure in the range of about 0.05–0.21 atm. The data obtained under normal used conditions of open circuit measurements are clearly underestimated, due to internal leakage through the mixed conductor and non-negligible electrode polarization. The errors increase with decreasing temperature, indicating that the temperature dependence of the exchange current density is stronger than for the actual leakage current results, as expected.

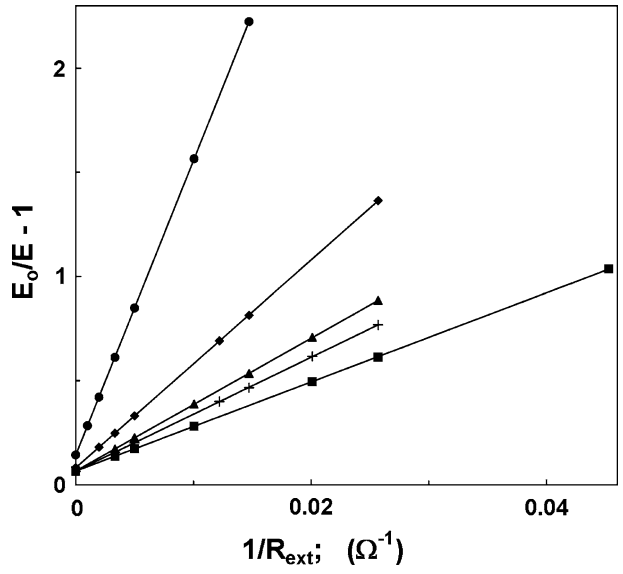

Fig. 6 The emf measurements obtained under external load conditions for $Gd_{1.9}Ca_{0.1}Ti_2O_{7-\delta}$ at 1,023, 1,073, 1,123, 1,173 and 1,223 K (from top to bottom)

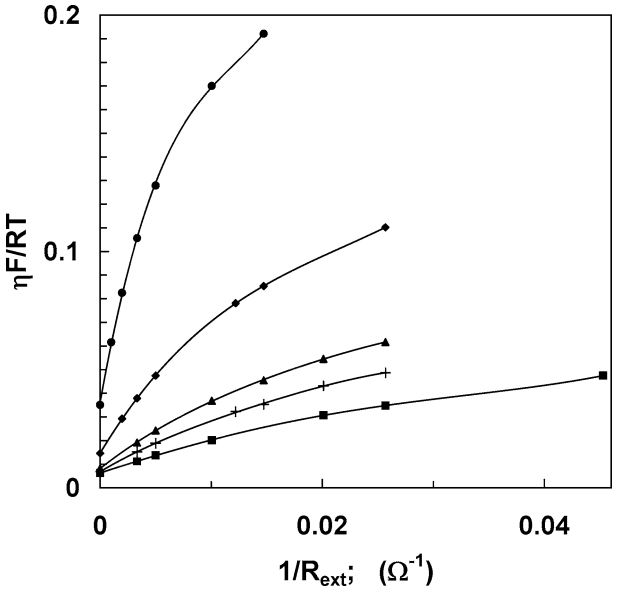

Fig. 8 Overpotential values extracted from emf measurements under external load conditions for $Gd_{1.9}Ca_{0.1}Ti_2O_{7-\delta}$ with porous Pt electrodes at 1,023, 1,073, 1,123, 1,173 and 1,223 K (from *top* to *bottom*).

The correctness of the measurements under external load conditions is indicated by the range of values of dimensionless overpotential $\eta F/RT < 0.2$ (Fig. 8), and also confirmed by the nearly linear dependence of overpotential on current density (Fig. 9), obtained as described by Eq. 9, with experimental results of E_o, E, and R_{ext}. The electronic and ionic resistance values were previously evaluated on combining results of total conductivity and the intercept to slope ratio of $E_o/E-1$ vs $1/R_{ext}$ (Eq. 2). Figure 9 thus validates the assumption that the polarisation resistance remains nearly constant for the actual working conditions, i.e., with the actual range of external load resistance.

Since the values of dimensionless overpotential ($\eta F/RT < 0.2$) correspond to a nearly linear dependence of overpotential on current density, Eq. 16 yields $AR_\eta \approx [(i_{oa}\, n_a)^{-1} + (i_{oc}\, n_c)^{-1}]RT/F$ hence:

$$[(i_{oa}n_a)^{-1} + (i_{oc}n_c)^{-1}]^{-1} \approx RT/(FR_\eta A), \tag{23}$$

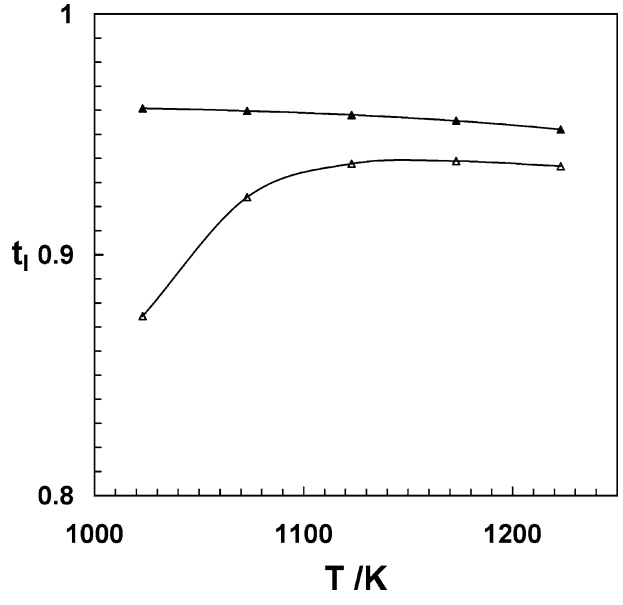

Fig. 7 The values of ionic transport number of $Gd_{1.9}Ca_{0.1}Ti_2O_{7-\delta}$ obtained by emf measurements under open-circuit conditions (*open symbols*) and under short-circuit conditions (*closed symbols*)

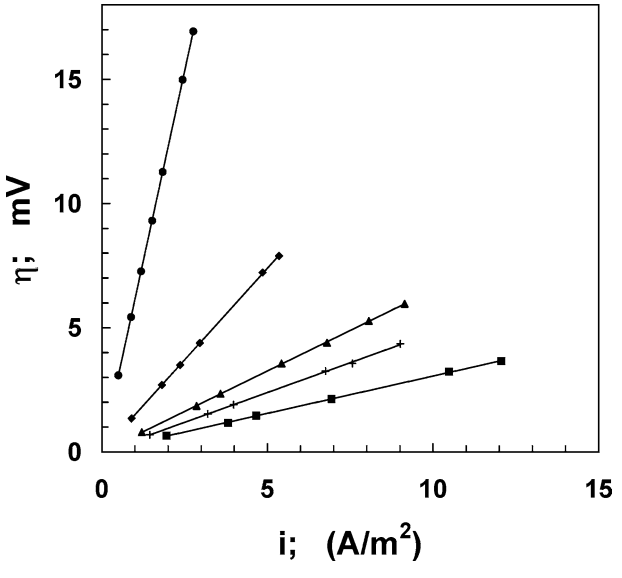

Fig. 9 Overpotential versus current dependencies extracted from emf measurements under short-circuit conditions for $Gd_{1.9}Ca_{0.1}Ti_2O_{7-\delta}$ with porous Pt electrodes at 1,023, 1,073, 1,123, 1,173 and 1,223 K (from *top* to *bottom*)

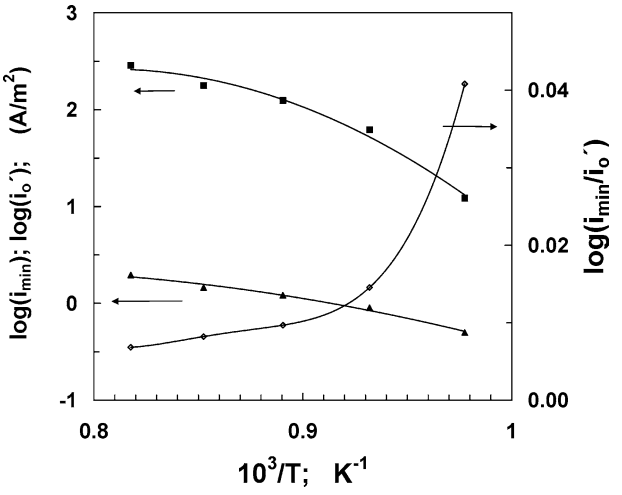

Fig. 10 Estimates of polarisation resistance and range of exchange current density

where the combination of both exchange current density values (i_{oa} or i_{oc}) represents an overall kinetic parameter.

The actual experiments were obtained for relatively low values of E_o when similar electrode kinetics can be expected at both sides of the concentration cell, except possibly for small differences in exchange current density, due to differences in oxygen chemical potential. We thus assumed the type of dependence reported for ceria-based materials, Eqs. 11 and 12. Note that both $Gd_{1.9}Ca_{0.1}Ti_2O_{7-\delta}$ [11] and ceria solid electrolytes [19, 20] possess a minor p-type conductivity contribution which decreases with decreasing pO_2. Under those conditions and for typical values $n_a = n_c = 2$, Eq. 23 yields

$$i'_o = 0.5\{1 + \exp[(E_o - \eta)F/RT]\}RT/(FR_\eta A). \quad (24)$$

This gives a typical range of exchange current density results under reference conditions (i.e. in air), and the results shown in Fig. 10 were computed for the values of overpotential under open circuit conditions, i.e. $\eta = E_o - E[1 + (R_I/R_e)]$. The exchange current density of the controlling electrode drops from about 3×10^2 A/m^2 at 1,223 K to about 12 A/m^2 at 1,023 K; this is still within the range of exchange current values which are sufficient to ensure the applicability of emf measurements under external load conditions, as shown by the simulated cases in Figs. 2 and 3.

The estimated range of exchange current values can also be used to assess the validity of the open-circuit emf estimates of the ionic transport number. Such measurements require reversible electrode kinetics, which implies that the exchange current density should be several orders of magnitude higher than the range of leakage current across the cell material. Its lowest value corresponds to open circuit conditions, i.e:

$$i_{min} = E/(AR_e) \quad (25)$$

The values of i_{min} and ratio i_{min}/i_o' are thus also shown in Fig. 10, to show that the assumption of reversible electrodes is arguable, thus explaining the differences between the corrected values of transport number obtained by emf measurements with external loading, and the corresponding open-circuit emf measurements (Fig. 7). The results shown in Fig. 10 also explain the increasing differences with decrease in temperature, based on the stronger temperature dependence of the exchange current density results. The ratio i_{min}/i_o' thus increases with decreasing temperature, indicating increasing deviations from reversible electrode kinetics. The actual conditions in Fig. 10 should correspond to values of oxygen partial pressure of about 0.05 atm, at the working electrode. We may assume faster kinetics at the reference electrode, which operates under more oxidising conditions ($\approx$ 0.21 atm).

Conclusions

Simulations of emf measurements under short-circuit conditions show that this method yields correct estimates of ionic transport number even for cases where the corresponding open-circuit measurements yield poor estimates of transport numbers. A criterion proposed to verify the applicability of emf results obtained under external load conditions is based on the values of dimensionless overpotential $F\eta/RT$. Nearly constant polarisation resistance $R_\eta = \eta/I$ can be expected when the values of $F\eta/RT$ remain smaller than approximately 0.2. Otherwise, we should only use sufficiently high values of external resistance to ensure that relative changes in current remain small. The most adverse conditions for the applicability of the emf measurements with external load conditions are for cases when the electrode kinetics is hindered by a relatively small limiting current density. We should thus avoid such conditions, and verify if the overpotential increases faster than current on varying the external load resistance. A study case is also presented to illustrate the applicability conditions for this method, and to explain the differences between the estimates of ionic transport number obtained by emf measurements under short-circuit and open-circuit conditions.

Acknowledgements This work was partially funded by the FCT, Portugal (contracts POCTI/CTM/39381/2001, BD/6827/2001 and BPD/11606/2002), and the NATO SfP979002 project.

References

1. Gorelov VP (1988) Elektrokhimiya 24:1380
2. Liu M, Hu H (1996) J Electrochem Soc 143:L109
3. Guan J, Dorris SE, Balachandran U, Liu M (1998) Solid State Ionics 110:303
4. Kim S, Wang S, Chen X, Yang YL, Wu N, Ignatiev A, Jacobson AJ, Abeles B (2000) J Electrochem Soc 147:2398
5. Kharton VV, Viskup AP, Kovalevsky AV, Figueiredo FM, Jurado JR, Yaremchenko AA, Naumovich EN, Frade JR (2000) J Mater Chem 10:1161

6. Stephens WT, Mazanec TJ, Anderson HU (2000) Solid State Ionics 129:271
7. Otter MW, Bouwmeester HJM, Boukamp BJ, Verweij H (2001) J Electrochem Soc 148:J1
8. Fielitz P, Borchardt G (2001) Solid State Ionics 144:71
9. Vashook VV, Daroukh M, Ullmann H (2001) Ionics 7:59
10. Kharton VV, Viskup AP, Figueiredo FM, Naumovich EN, Yaremchenko AA, Marques FMB (2001) Electrochim Acta 46:2879
11. Kharton VV, Marques FMB (2001) Solid State Ionics 140:381
12. Kharton VV, Tsipis EV, Yaremchenko AA, Vyshatko NP, Shaula AL, Naumovich EN, Frade JR (2003) J Solid State Electrochem 7:468
13. Patterson JW (1979) In: Brubaker G et al. (eds) ACS symposium series, no. 89, Corrosion Chemistryp. 96, American Chemical Society, Washington DC, pp 96
14. Riess I (1992) In: Balkanski M, Takahashi T, Tuller HL (eds) Solid state ionics. Elsevier, Amsterdam, pp 475
15. Wang DY, Nowick AS (1979) J Electrochem Soc 126:1155
16. Kenjo T, Horiuchi Y, Osawa S (1990) J Electrochem Soc 137:2423
17. Marques FMB, Wirtz GP (1992) J Amer Ceram Soc 75:369
18. Wirtz GP, Marques FMB (1992) J Amer Ceram Soc 75:375
19. Lubke S, Wiemhofer HD (1999) Solid State Ionics 117–229
20. Fagg DP, Abrantes JCC, Coll DP, Nuñez P, Kharton VV, Frade JR (2003) Electrochim Acta 48:1023